# Accepted Manuscript

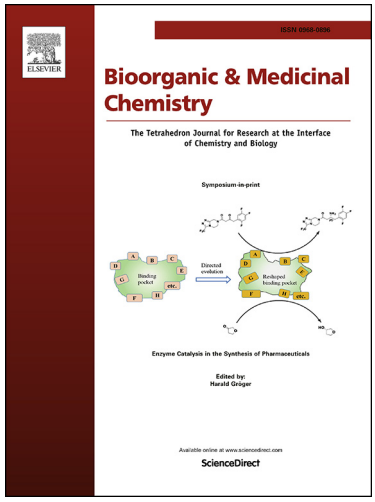


4-(3-Alkyl-2-oxoimidazolidin-1-yl)-*N*-phenylbenzenesulfonamides as new antimitotic prodrugs activated by cytochrome P450 1A1 in breast cancer cells

Atziri Corin Chavez Alvarez, Mitra Zarifi Khosroshahi, Marie-France Côté, Mathieu Gagné-Boulet, Sébastien Fortin

PII: S0968-0896(18)31159-3
DOI: https://doi.org/10.1016/j.bmc.2018.09.001
Reference: BMC 14526

To appear in: *Bioorganic & Medicinal Chemistry*

Received Date: 20 June 2018
Revised Date: 24 August 2018
Accepted Date: 2 September 2018

Please cite this article as: Alvarez, A.C.C., Khosroshahi, M.Z., Côté, M-F., Gagné-Boulet, M., Fortin, S., 4-(3-Alkyl-2-oxoimidazolidin-1-yl)-*N*-phenylbenzenesulfonamides as new antimitotic prodrugs activated by cytochrome P450 1A1 in breast cancer cells, *Bioorganic & Medicinal Chemistry* (2018), doi: https://doi.org/10.1016/j.bmc.2018.09.001

# 4-(3-Alkyl-2-oxoimidazolidin-1-yl)-*N*-phenylbenzenesulfonamides as new antimitotic prodrugs activated by cytochrome P450 1A1 in breast cancer cells

Atziri Corin Chavez Alvarez, Mitra Zarifi Khosroshahi, Marie-France Côté, Mathieu Gagné-Boulet and Sébastien Fortin*

CHU de Québec-Université Laval Research Center, Oncology Division, Hôpital Saint-François d'Assise, 10 rue de l'Espinay, Quebec City, QC, G1L 3L5, Canada.

Faculty of Pharmacy, Laval University, Quebec City, QC, G1V 0A6, Canada.

***Corresponding author:** Sébastien Fortin, Phone: 418-525-4444 ext. 52364, Fax: 418-525-4372, e-mail: sebastien.fortin@pha.ulaval.ca.

**Declarations of interest:** none

**Abbreviations:** phenyl 4-(2-oxo-3-alkylimidazolidin-1-yl)benzenesulfonates, PAIB-SOs; cytochromes P450, CYPs; 4-(3-alkyl-2-oxoimidazolidin-1-yl)-*N*-phenylbenzenesulfonamides, PAIB-SAs; phenyl 4-(2-oxoimidazolidin-1-yl)benzenesulfonates, PIB-SOs; phenyl 4-(2-oxoimidazolidin-1-yl)benzenesulfonamides, PIB-SAs.

**ABSTRACT**

The role and the importance of the sulfonate moiety in phenyl 4-(2-oxo-3-alkylimidazolidin-1-yl)benzenesulfonates (PAIB-SOs) were assessed using its bioisosteric sulfonamide equivalent leading to new cytochrome P450 1A1 (CYP1A1)-activated prodrugs designated as 4-(3-alkyl-2-oxoimidazolidin-1-yl)-*N*-phenylbenzenesulfonamides (PAIB-SAs). PAIB-SAs are active in the submicromolar to low micromolar range showing selectivity toward CYP1A1-expressing MCF7 cells as compared to cells devoid of CYP1A1 activity such as MDA-MB-231 and HaCaT cells. The most potent PAIB-SA **13** bearing a trimethoxyphenyl group on ring B blocks the cell cycle progression in G2/M phase, disrupts the microtubule dynamics and is biotransformed by CYP1A1 into CEU-638, its potent antimicrotuble counterpart. Structure-activity relationships related to PAIB-SOs and PAIB-SAs evidenced that PAIB-SOs and PAIB-SAs are true bioisosteric equivalents fully and selectively activatable by CYP1A-expressing cells into potent antimitotics.

**Keywords:** Antimicrotubule agents; Antimitotics; CYP1A1-activated prodrugs; 4-(3-Alkyl-2-oxoimidazolidin-1-yl)-*N*-phenylbenzenesulfonamides; PAIB-SAs

## 1. Introduction

Breast cancer accounts for 25% of all women cancer cases and 15% of all women cancer deaths, making it by far the most common cancer and the leading cause of cancer death among women worldwide.[1] According to the American Cancer Society, it is estimated in the USA in 2018 that 266,120 new cases of invasive breast cancer will be diagnosed in women and 41,400 breast cancer deaths will occur.[2] Despite advances in the treatment of early-stage disease, approximately 40% of patients will experience recurrence and develop resistance to antihormone therapy and anticancer agents.[3, 4] This results in more aggressive breast cancer, more difficult to treat and it becomes life threatening.[5] Therefore, the 5-year relative survival rate for women diagnosed with localized breast cancer is 98.6% and it declines to 23.3% for cancers at distant stages.[6] Consequently, breast cancer is among the most pressing health problems worldwide and for that reason new therapeutic options and strategies are intensively sought.

Cytochromes P450 (CYPs) are a large superfamily of heme-containing monooxygenase enzymes. In humans, there are 18 families and 43 subfamilies of CYPs encoded by 57 genes.[7] CYPs metabolize a large number of structurally different endogenous and exogenous compounds such as steroids, fatty acids, prostaglandins and plant metabolites. They also metabolize chemical carcinogens, mutagens and other environmental contaminants.[8] They are the main enzymes involved in drug metabolism accounting for the metabolism of approximately 75% of marketed drugs.[9] CYPs are ubiquitous but are predominantly expressed in the liver and to a lesser extent in the small intestine, lungs, placenta and kidneys.[10] Some CYPs such as CYP3A4, 2D6, 2C19 and 2C9 are not specific metabolizing a wide variety of compounds while others such as CYP17A1 and 19A1 are more specific and are expressed in specific tissues such as ovarian follicles as well as in fetal tissues.[11] Therefore, the expression level of CYP varies according to their roles and tissues in which they are expressed.[12, 13] There is also evidence that some CYPs are differentially expressed in tumors cells versus their healthy counterparts.[14-16] CYP isoforms such as CYP1A1 are expressed in tumors and represent valuable therapeutic targets that may influence

tumor response to current antineoplastics.[15-17] To that end, that concept has been applied to benzothiazole and aminoflavone exemplified by Phortress (**1**) and NSC710464 (**2**) that are prodrugs of alkylating agents activated by CYP1A1 (Fig. 1).[18, 19]

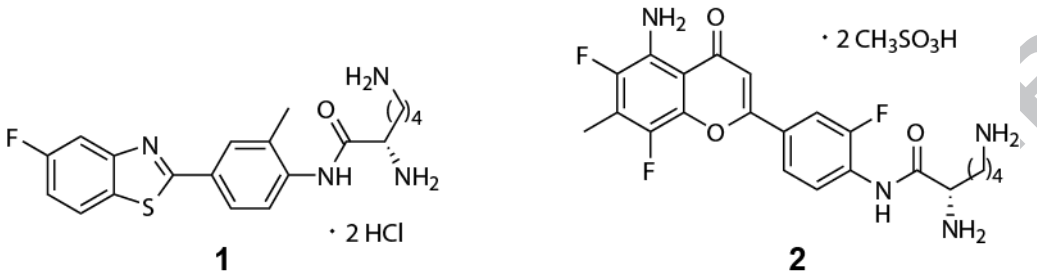


**Figure 1.** Molecular structure of CYP1A1-activated benzothiazole Phortress (**1**) and aminoflavone NSC710464 (**2**).

CYP1A1 is one of the three members of the CYP1 family (CYP1A1, 1A2 and 1B1). In normal conditions, CYP1A1 is predominantly detected in extrahepatic tissues at a very low level but it can be induced significantly by several xenobiotics under the control of the ligand-activated aryl hydrocarbon receptor.[20-22] Studies have shown that most breast tumors express CYP1A1 but CYP1A1 seems to be detected only at a low level in the normal surrounding tissues.[23-26] Moreover, CYP1A1 is involved in the regulation of breast cancer cell proliferation and survival and correlates positively with the tumor grade.[26] In this context, the use of CYP1A1 as a druggable target to design anticancer prodrugs represents a promising and attractive strategy to develop new targeted therapy for breast cancer treatment.

To this end, we recently developed a new family of anticancer agents designated as phenyl 4-(2-oxo-3-alkylimidazolidin-1-yl)benzenesulfonates (PAIB-SOs, Fig. 2) represented by the prototypical 3,4,5-trimethoxyphenyl 4-(3-butyl-2-oxoimidazolidin-1-yl)-benzenesulfonate (CEU-818) that are highly selective toward several breast cancer cell lines notably MCF7 cells.[27] They block the cell cycle progression in the G2/M phase and disrupt the microtubule network of sensitive breast cancer cells. PAIB-SOs were rationally designed as CYP1A1-activated prodrugs of antimitotics designated as phenyl

4-(2-oxoimidazolidin-1-yl)benzenesulfonates (PIB-SOs, Fig. 2).[28] To the best of our knowledge, PAIB-SOs are the first antimitotic prodrugs to be reported that are activated by CYP1A1. On the one hand, our structure-activity relationship studies showed that PAIB-SOs must be substituted by a propyl or butyl group on the phenylimidazolidinone moiety of the aromatic ring A as well as by methoxyl or halogen group at positions 3, 4, and/or 5 of the aromatic ring B to maintain both antiproliferative activity and selectivity toward breast cancer cells.[27] On the other hand, we found that the sulfonate group of PIB-SOs, the cytotoxic antimitotic metabolites of PAIB-SOs, retains its cytocidal and antimicrotubule activities when replaced by a sulfonamide group. This led to antimitotic PIB-SO analogs designed as phenyl 4-(2-oxoimidazolidin-1-yl)benzenesulfonamides (PIB-SAs, Fig. 2) represented by the prototypical 4-(2-oxoimidazolidin-1-yl)-*N*-(3,4,5-trimethoxyphenyl)benzenesulfonamide (CEU-638).[29]

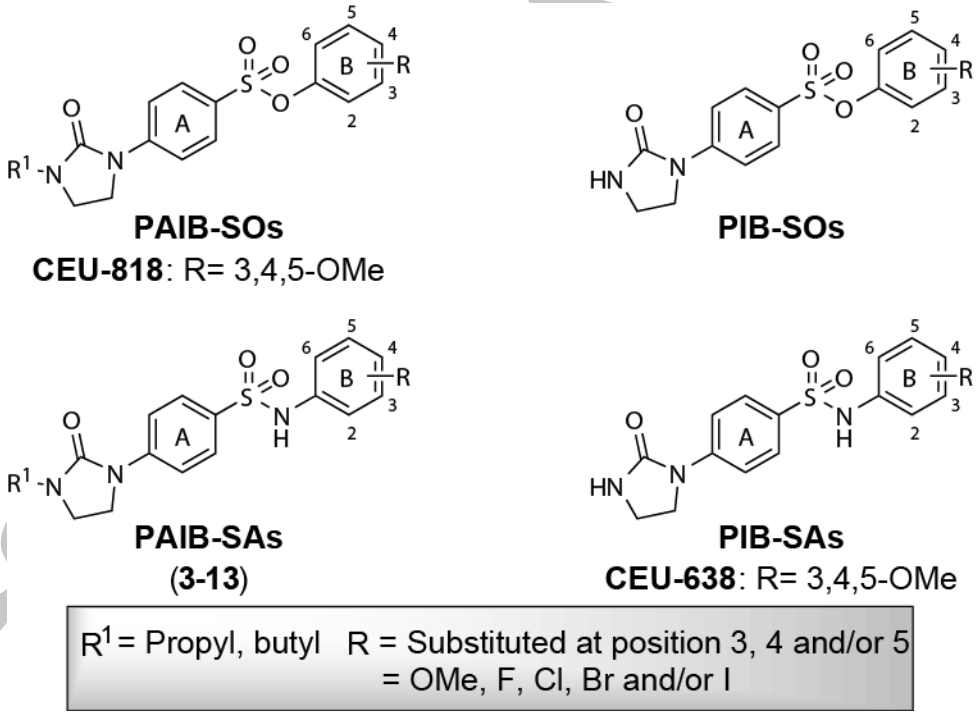


**Figure 2.** Molecular structure of CYP1A1-activated prodrugs phenyl 4-(2-oxo-3-alkylimidazolidin-1-yl)benzenesulfonates (PAIB-SOs) and 4-(3-alkyl-2-oxoimidazolidin-1-yl)-N-phenylbenzenesulfonamides (PAIB-SAs) as well as antimitotics phenyl 4-(2-oxoimidazolidin-1-

yl)benzenesulfonates (PIB-SOs) and phenyl 4-(2-oxoimidazolidin-1-yl)benzenesulfonamides (PIB-SAs).

Herein, we studied the conversion of the sulfonate moiety of PAIB-SOs into its bioisosteric sulfonamide equivalent on the cytocidal activity and the selectivity toward CYP1A1-expressing MCF7 breast cancer cells. To that end, a series of 11 PAIB-SAs was designed and prepared where the sulfonate moiety of PAIB-SOs was replaced by a sulfonamide group. Thereafter, the antiproliferative activity of PAIB-SAs was assessed on sensitive CYP1A1-expressing MCF7 breast cancer cells and two insensitive cell lines devoid of CYP1A1; one human breast cancer cell line (MDA-MB-231 carcinoma) and one healthy primary cell line (HaCaT, epidermal keratinocytes). Then, the most potent and selective compound was assessed for its ability to block the cell cycle progression in the G2/M phase, to disrupt the microtubule network and to be activated into its antimitotic counterpart by CYP1A1.

**2. Chemistry**

The method used for the preparation of PAIB-SAs (**3-13**) is described in Scheme 1. Compound **16** was prepared as published previously.[27] Briefly, the synthesis of 1-phenylimidazolidin-2-one (**14**) was achieved by the nucleophilic addition of aniline to 2-chloroethyl isocyanate in methylene chloride at 25 °C followed by the intramolecular cyclization of the 1-(2-chloroethyl)-3-phenylurea using sodium hydride in THF at 25 °C. Thereafter, 1-butyl-3-phenylimidazolidin-2-one (**15**) was obtained by the addition of 1-iodobutane to a solution of **14** and sodium hydride in tetrahydrofuran. Then, 4-(3-butyl-2-oxoimidazolidin-1-yl)benzenesulfonyl chloride (**16**) was prepared by the chlorosulfonation of compound **15** using chlorosulfonic acid in carbon tetrachloride at 0 °C. Finally, PAIB-SAs **3-13** were obtained by nucleophilic addition of either 2-methoxyaniline, 3-methoxyaniline, 3-fluoroaniline, 3-bromoaniline, 3-iodoaniline, 3,4-dimethoxyaniline, 3,4-difluoroaniline, 3,5-dimethoxyaniline, 3,5-difluoroaniline, 3,5-

dichloroaniline or 3,4,5-trimethoxyaniline to sulfonyl chloride **16** in the presence of 4-dimethylaminopyridine in dry acetonitrile at 25 °C.

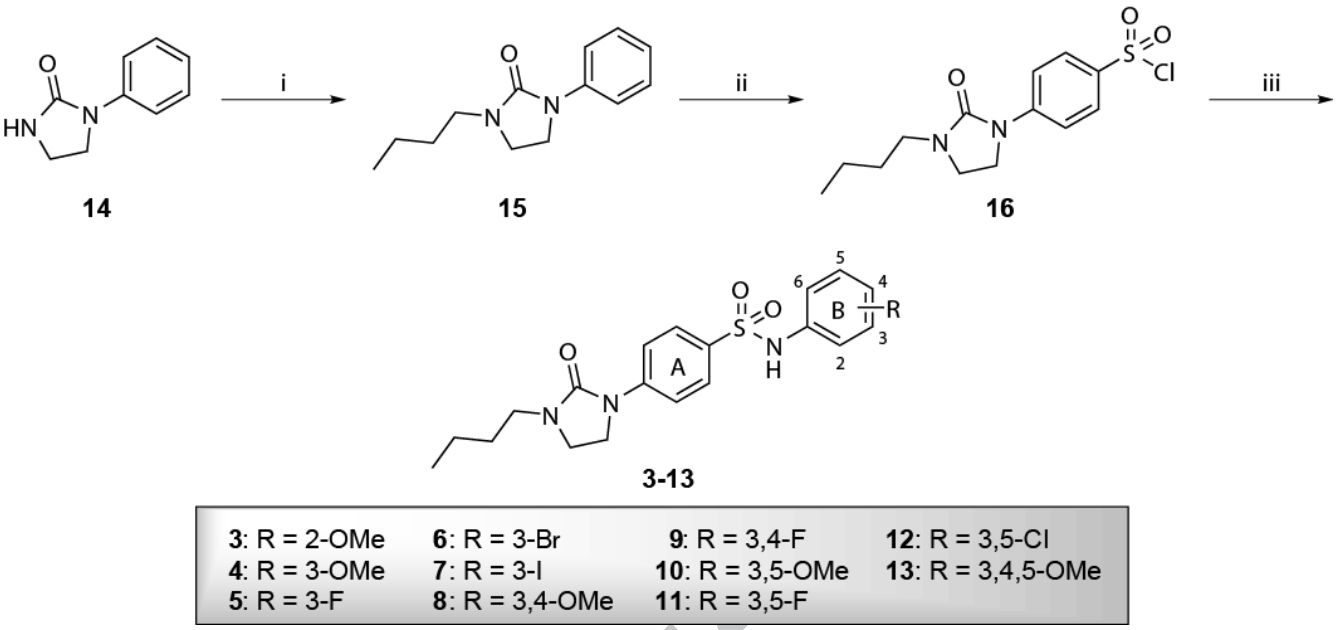


| | | | |
|---|---|---|---|
| **3**: R = 2-OMe | **6**: R = 3-Br | **9**: R = 3,4-F | **12**: R = 3,5-Cl |
| **4**: R = 3-OMe | **7**: R = 3-I | **10**: R = 3,5-OMe | **13**: R = 3,4,5-OMe |
| **5**: R = 3-F | **8**: R = 3,4-OMe | **11**: R = 3,5-F | |

**Scheme 1.** Reagent conditions: i) NaH, 1-iodobutane, THF, 0 °C to R.T.; ii) $ClSO_3H$, $CCl_4$, 0 °C; iii) relevant aniline, DMAP/$CH_3CN$, R.T.

## 3. Results and discussion

Our previous study showed that MCF7 breast cancer cells are expressing CYP1A1 and are sensitive to PAIB-SOs while MDA-MB-231 breast cancer cells are devoid of CYP1A1 activity and are insensitive to PAIB-SOs.[27] In this context, the antiproliferative activity of PAIB-SAs was assessed on sensitive MCF7 cells, on insensitive MDA-MB-231 cells and on healthy primary HaCaT epidermal keratinocyte cells in the aim to confirm that PAIB-SAs act similarly to PAIB-SOs and that they are not cytotoxic on healthy cells. Antiproliferative activity was assessed according to the NCI/NIH Developmental Therapeutics Program.[30] The PIB-SA bearing a 3,4,5-trimethoxyl group on ring B (CEU-638) and combretastatin A-4 (CA-4) were used as positive controls. The results are summarized in Table 1 and they are expressed as the concentration of drug inhibiting cell growth by 50% ($IC_{50}$). The structure-

activity relationships related to PAIB-SAs show a similar trend to those obtained with PAIB-SOs. First, except for compound **12**, all PAIB-SAs substituted by methoxyl and halogen groups at positions 2, 3, 4, and/or 5 of the aromatic ring B exhibit an antiproliferative activity in the submicromolar to low micromolar range on MCF7 cells (0.25 to 3.1 μM) and show a selectivity ratio between > 5.3 and 372 (HaCaT/MCF7 cells). Compounds **6**, **8** and **13** bearing either a 3-bromo, 3,4-dimethoxyl or a 3,4,5-trimethoxyl group on the aromatic ring B are the most potent and selective compounds showing antiproliferative activity between 0.25 and 0.68 μM and displaying selectivity ratio between > 147 and 372 (HaCaT/MCF7 cells). Interestingly, the antiproliferative activity difference between PAIB-SOs and PAIB-SAs is in the same order of magnitude as the difference between PIB-SOs and PIB-SAs.[27-29] Compound **13** bearing a 3,4,5-trimethoxyl group is the most potent and selective on MCF7 cells and it was selected for further studies to confirm its mechanism of action.

**Table 1.** Antiproliferative activity ($IC_{50}$) of PIB-SAs (**3-13**), CEU-818, CEU-638 and CA-4 on MCF7, MDA-MB-231 and HaCaT cells as well as their selectivity ratio toward sensitive MCF7 breast cancer cells compared to primary HaCaT epidermal keratinocytes.

| # | $IC_{50}$ (μM)[1] | | | Selectivity Ratio[2] |
|---|---|---|---|---|
| | **MCF7** | **MDA-MB-231** | **HaCaT** | **HaCaT/ MCF7** |
| **3** | 1.6 | > 100 | > 100 | > 63 |
| **4** | 1.1 | > 10 | > 10 | > 9.1 |
| **5** | 0.78 | > 50 | > 50 | > 64 |
| **6** | 0.28 | 83 | 51 | 182 |
| **7** | 0.54 | > 100 | 21 | 39 |
| **8** | 0.68 | > 100 | > 100 | > 147 |
| **9** | 1.9 | > 10 | > 10 | > 5.3 |
| **10** | 2.6 | > 100 | 58 | 22 |
| **11** | 3.1 | > 50 | > 50 | > 16 |
| **12** | > 10 | > 10 | > 10 | N.A. |
| **13** | 0.25 | 27 | 93 | 372 |
| **CEU-638** | 0.022 | 0.038 | 0.019 | 0.86 |
| **CEU-818**[27] | 0.0055 | 6.0 | > 10 | > 1800 |
| **CA-4**[3] | 0.0021 | 0.0024 | 0.0014 | 0.67 |

[1]$IC_{50}$ is expressed as the concentration of drug inhibiting cell proliferation by 50% after 72 h of treatment. When 100 μM is not attained, the maximum concentration assessed represents the maximum solubility concentration reached in complete medium containing DMSO 0.5%. [2]Selectivity ratio is expressed as the ratio of the $IC_{50}$ value found in primary HaCaT cells to that measured in sensitive MCF7 cells. N.A., not applicable. [3]CA-4, combretastatin A-4.

The lag time to the onset of antiproliferative action on cancer cells is an important parameter to be assessed prior to *in vivo* assays. The time required by PAIB-SA **13** to induce its antiproliferative activity was thus evaluated on MCF7 cells. The PIB-SA antimitotic counterpart CEU-638 was used as positive control. As shown in Fig. 3, the antiproliferative activity of compound **13** at high concentrations is similar either at 24, 36 or 48 h to CEU-638. Our results confirm that the antiproliferative activity is time-dependent. The incubation of the drug with the cells for at least 24h is required to affect cell proliferation.

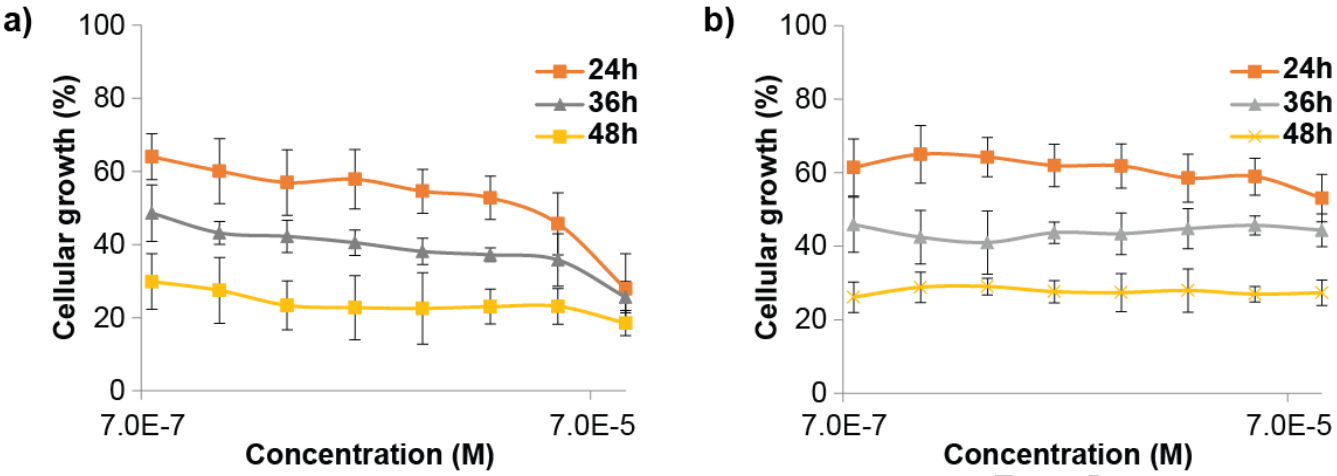


**Figure 3.** Dose-dependent antiproliferative activity of a) compound **13** and b) its parental antimitotic drug CEU-638 at 24, 36 and 48 h on MCF7 cells.

On one hand, it is known that PAIB-SOs that are the bioisosteric equivalents of PAIB-SAs and that they are activated in CYP1A1-expressing cells into the highly potent antimitotics PIB-SOs.[27, 28] On the other hand, PIB-SAs are also known to exhibit potent antimicrotubule effects on a large number of cancer cell lines.[29] Therefore, we hypothesized that PAIB-SAs are activated into PIB-SAs by CYP1A1 relevant cancer cells leading to G2/M phase arrest and disruption of the microtubule dynamics that triggers anoikis. To confirm our hypothesis, PAIB-SA **13** was assessed for its effect on cell cycle progression and cytoskeleton integrity in sensitive MCF7 cells. As shown in Fig. 4, MCF7 cells treated with 0.5% DMSO were found in subG1, G0/G1, S, and G2/M phases at 2.9, 69, 15.1 and 13%, respectively. Compound **13** strongly blocks the cell cycle progression in G2/M phase increasing the number of cells in G2/M phase by 17.2 and 29.4% at 0.20 and 0.50 μM, respectively which is similar to that obtained for CEU-638 and CA-4 used as positive controls where the number of cells in G2/M phase was increased by 33.7 and 32.9%, respectively. As shown in Fig. 5, the treatment of sensitive MCF7 cells by PAIB-SA **13** at 0.20 μM for 24 h leads to the disruption of the cytoskeleton equivalently to CEU-638 and CA-4 used as positive controls.

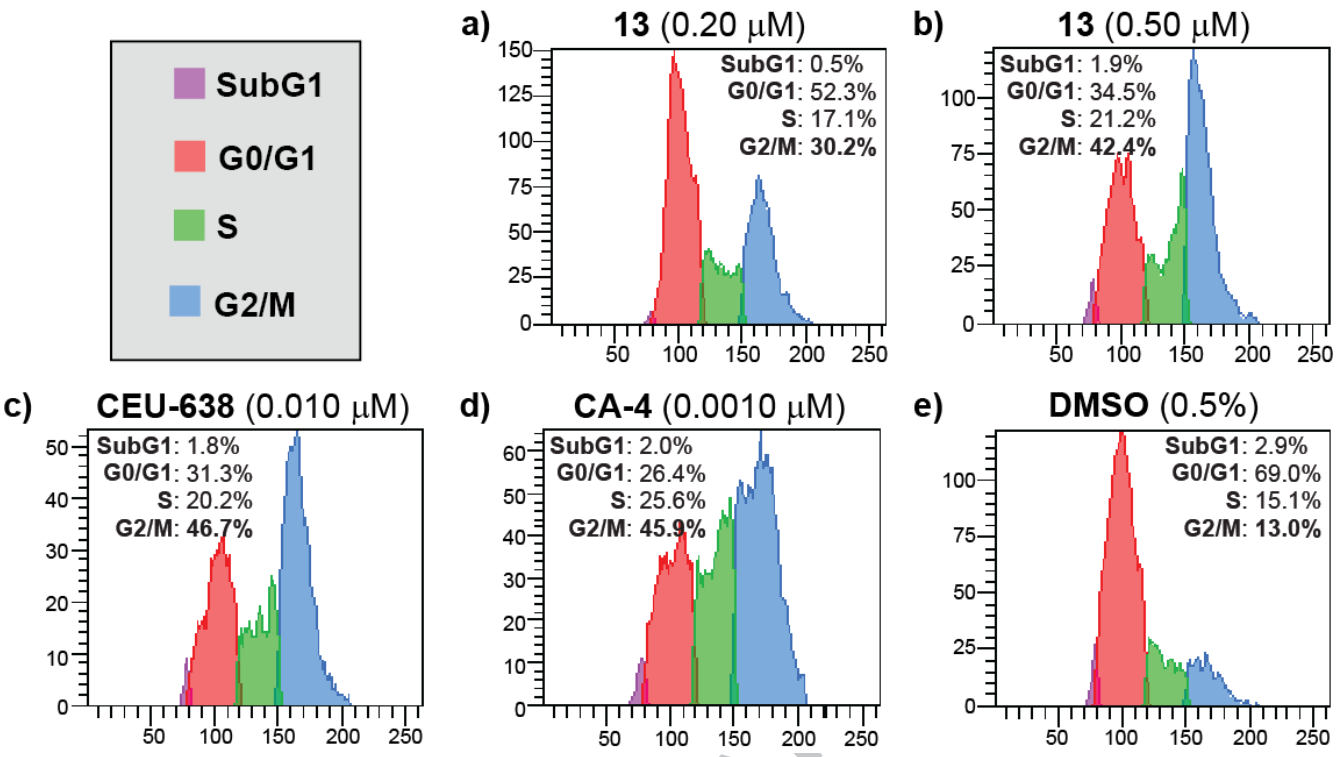


**Figure 4.** Effect on the cell cycle progression on MCF7 cells after a 24 h treatment with a) PAIB-SA **13** (0.20 μM), b) PAIB-SA **13** (0.50 μM), c) CEU-638 (0.010 μM), d) CA-4 (0.0010 μM) and e) DMSO (0.5%).

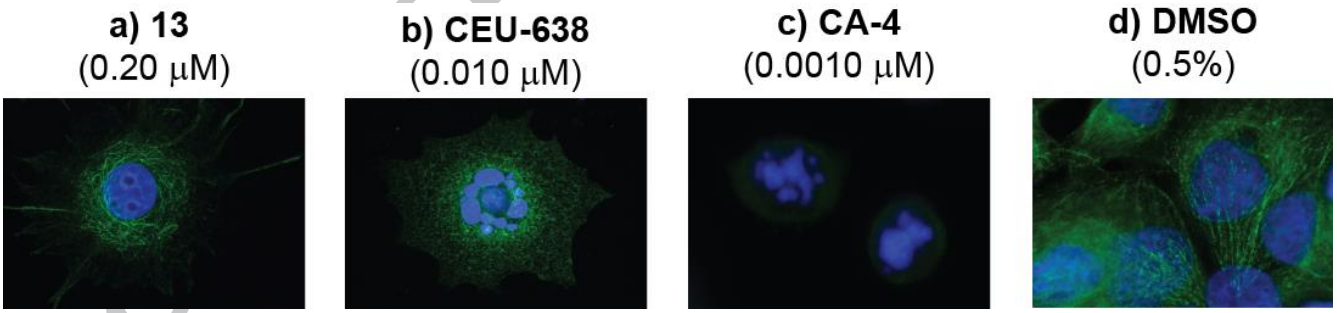


**Figure 5.** Effect of a) PAIB-SA **13** (0.20 μM), b) CEU-638 (0.010 μM), c) CA-4 (0.0010 μM) and d) DMSO 0.5% on cytoskeleton integrity in MCF7 cells after 24 h of treatment.

To confirm that the PAIB-SAs exhibit the same mechanism of activation observed for PAIB-SOs and that they are CYP1A1-activated prodrugs, 1.2 μM of PAIB-SA **13** was incubated in presence of CYP1A1

Supersomes$^{TM}$ for 0, 15, 30, 60, 90, 120 and 150 min, respectively. Afterward, the metabolites were identified by HPLC-UV. CEU-638, the parental antimitotic drug of **13** was used as internal standard. As shown in Fig. 6, CYP1A1 Supersomes$^{TM}$ activated PAIB-SA **13** into its parental antimitotic CEU-638. Altogether, these results confirm the bioisosterism of sulfonate and sulfonamide groups and that PAIB-SAs are a new class of CYP1A1-activated prodrugs exhibiting a similar mechanism of activation that their PAIB-SOs structural analogs.

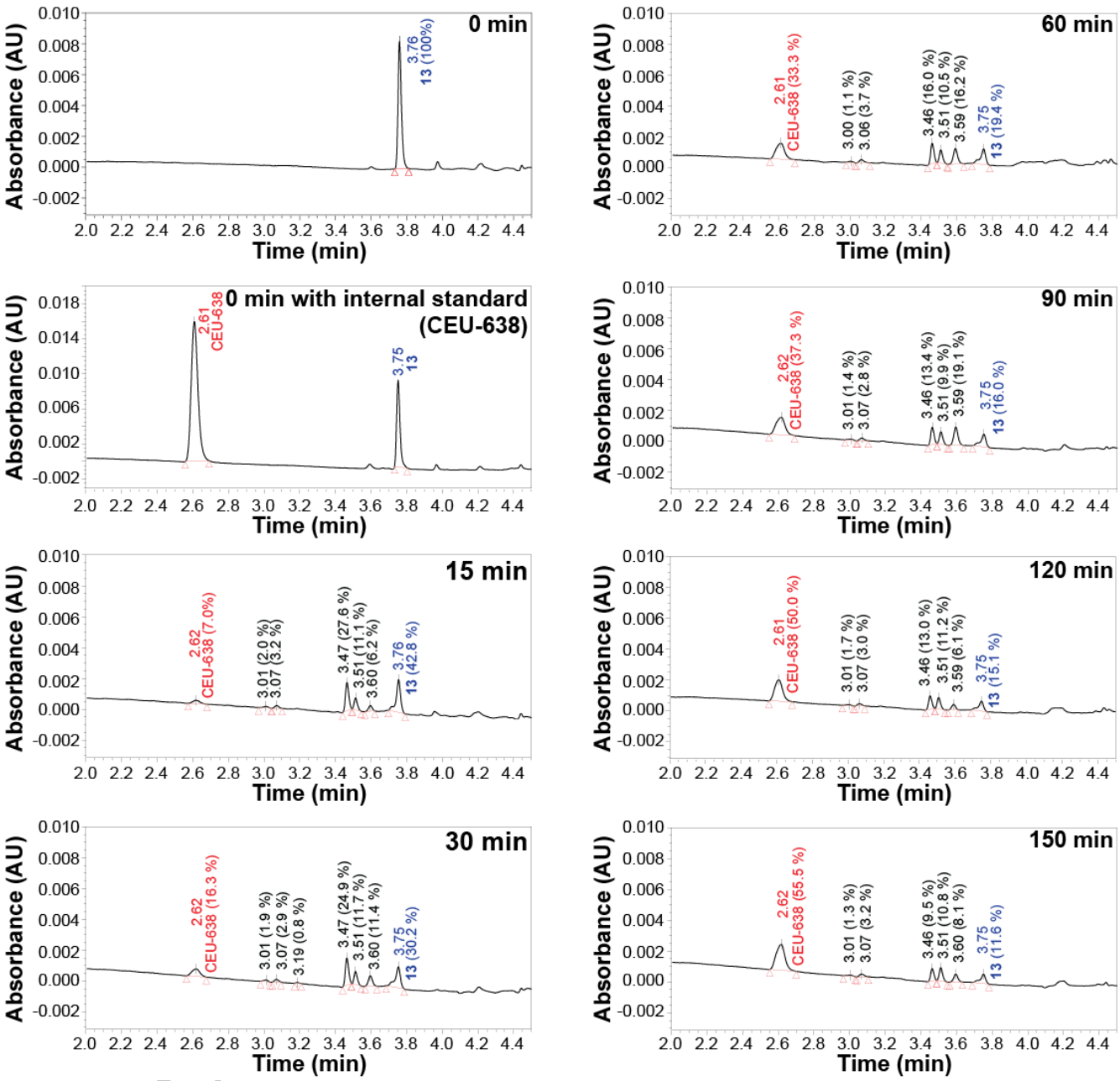


**Figure 6.** The time-course activation of PAIB-SA **13** into PIB-SA CEU-638 by CYP1A1.

## 4. Conclusion

In summary, we have shown that the newly designed PAIB-SAs are active in the submicromolar to low micromolar range and selective toward MCF7 breast cancer cells comparatively to MDA-MB-231 and HaCaT cells. Using the most potent PAIB-SA **13**, we found that it blocks the cell cycle progression in

the G2/M phase and disrupts the microtubule dynamics efficiently. Finally, PAIB-SAs are activated by CYP1A1 confirming that 1) PAIB-SAs are CYP1A1-activated antimitotic prodrugs and 2) that sulfonate and sulfonamide groups are bioisosteric equivalents. Altogether, these results show that the structural bridge between the two aromatic rings might be investigated to improve the pharmacological and the physicochemical properties of this new class of promising antimitotic CYP1A1-activated prodrugs.

## 5. Experimental section

### *5.1. Chemistry*

#### *5.1.1. General*

Proton NMR spectra were recorded on a Bruker AM-300 spectrometer (Bruker, Germany). Chemical shifts (δ) are reported in parts per million (ppm). Uncorrected melting points were determined on an electrothermal melting point apparatus. HPLC analyses were performed using a Prominence LCMS-2020 system with binary solvent equipped with an UV/vis photodiode array and an APCI probe (Shimadzu, Columbia, MD). Compounds were eluted within 25 min on an Alltech Alltima C18 reversed-phase column (5 mm, 250 mm x 4.6 mm) equipped with an Alltech Alltima C18 precolumn (5 mm, 7.5 mm x 4.6 mm) with a MeOH/$H_2O$ linear gradient at 1.0 mL/min. Some HPLC analyses were also performed using an ACQUITY Arc system (Waters, Mississauga, Ontario). The purity of all final compounds was >95%. HRMS were recorded by direct injection in a TOF system 6210 series mass spectrometer (Agilent technologies, Santa Clara, CA). All chemicals were supplied by Aldrich Chemicals (Milwaukee, WI), Fisher Scientific (Toronto, ON, Canada) or VWR International (Mont-Royal, QC, Canada) and used as received unless specified otherwise. Liquid flash chromatography was performed on silica gel F60, 60 Å, 40-63 μm supplied by Silicycle (Québec, QC, Canada) using an FPX flash purification system (Biotage, Charlottesville, VA), and using solvent mixtures expressed as v/v ratios. Solvents and reagents were used without purification unless specified otherwise. The progress of all reactions was monitored

by TLC on precoated silica gel 60 F254 TLC plates (VWR). The chromatograms were viewed under UV light at 254 and/or 265 nm.

### *5.1.2. General procedure for preparation of compounds 14-16*

1-Phenylimidazolidin-2-one (**14**) was obtained by nucleophilic addition of aniline on 2-chloroethyl isocyanate followed by an intramolecular cyclization using sodium hydride as described previously by Fortin *et al.*[28, 29] Briefly, 2-chloroethyl isocyanate (1.2 eq.) was added dropwise to a cold solution (ice bath) of aniline (1.0 eq.) in dry methylene chloride (15 mL per g of aniline). The reaction mixture was stirred at room temperature for 24 h and the solvent was evaporated under reduced pressure. The white solid obtained was triturated twice in cold hexanes/methylene chloride 10:1. Thereafter, 1-(2-chloroethyl)-3-phenylurea (1 eq.) was dissolved in dry tetrahydrofuran under dry nitrogen atmosphere and the solution is cooled to 0 °C. Then, sodium hydride (3 eq.) was slowly added, the ice bath was removed after 30 min and the reaction mixture was stirred at room temperature for 5 h. The reaction mixture was quenched at 0 °C with water and diluted with ethyl acetate. The organic layer was washed with water and brine, dried over sodium sulfate, filtered and concentrated under reduced pressure to provide 1-phenylimidazolidin-2-one (**14**), which was used without further purification. 4-(3-Butyl-2-oxoimidazolidin-1-yl)benzenesulfonyl chloride (**16**) was synthesized using the method described by Fortin *et al.*[27]. Briefly, sodium hydride (1 eq.) was added slowly to a cold solution (ice bath) of **14** (30 mmol) in dry tetrahydrofuran. The ice bath was removed after 30 min. Thirty-six mmol of 1-iodobutane were then added slowly and the reaction mixture stirred at room temperature for 20 h. The reaction was quenched at 0 °C with water and the mixture diluted with EtOAc. The organic layer was washed with water and brine, dried over sodium sulfate, filtered, and concentrated under reduced pressure. The residue was purified by flash chromatography $CH_2Cl_2$ to $CH_2Cl_2$/EtOAc (9:1) to give an off-white solid. Afterwards, 1-butyl-3-phenylimidazolidin-2-one (**15**) was added slowly to chlorosulfonic acid (23.1 mmol) in $CCl_4$ (5 mL) at 0 °C for 2 h. Then, the reaction mixture was poured slowly into ice-water and

then filtered to collect the solid thus formed. The latter solid was dried overnight under reduced pressure to provide 4-(3-butyl-2-oxoimidazolidin-1-yl)benzenesulfonyl chloride (**16**) as a white solid.

### *5.1.3. Preparation and characterization of compounds 3-13*

Compound **16** (1.00 mmol) was suspended in dry acetonitrile (10 mL) under nitrogen atmosphere. Either 2-methoxyaniline, 3-methoxyaniline, 3-fluoroaniline, 3-bromoaniline, 3-iodoaniline, 3,4-dimethoxyaniline, 3,4-difluoroaniline, 3,5-dimethoxyaniline, 3,5-difluoroaniline, 3,5-dichloroaniline or 3,4,5-trimethoxyaniline (1.00 mmol) and 4-dimethylaminopyridine (4.00 mmol) were successively added dropwise to the suspension of **16**. The mixture was stirred at room temperature for 48 h and then diluted with ethyl acetate. The resulting solution was washed with hydrochloric acid 1N, brine, dried over sodium sulfate, filtered, and evaporated to dryness under reduced pressure. The white solid was purified by flash chromatography on silica gel.

5.1.2.2. 4-(3-Butyl-2-oxoimidazolidin-1-yl)-*N*-(2-methoxyphenyl)benzenesulfonamide (**3**). Flash chromatography (Hex to Hex/EtOAc (50:50)). Yield, 67%; white solid; mp: 141-143 °C. $^{1}$H NMR ($CDCl_3$): δ 7.67-7.64 (m, 2H, Ar), 7.56-7.53 (m, 2H, Ar), 7.48 (d, 1H, J = 7.7 Hz, Ar), 7.01 (s, 1H, NH), 6.98-6.96 (m, 1H, Ar), 6.85 (t, 1H, J = 7.7 Hz, Ar), 6.71-6.68 (m, 1H, Ar), 3.76-3.71 (m, 2H, $CH_2$), 3.63 (s, 3H, $CH_3$), 3.49-3.43 (m, 2H, $CH_2$), 3.26 (t, 2H, J = 7.3 Hz, $CH_2$), 1.55-1.46 (m, 2H, $CH_2$), 1.39-1.29 (m, 2H, $CH_2$), 0.92 (t, 3H, J = 7.3 Hz, $CH_3$). $^{13}$C NMR ($CDCl_3$): δ 157.0, 149.4, 144.6, 131.2, 128.3, 126.0, 125.2, 121.0, 120.8, 116.0, 110.6, 55.7, 43.6, 42.1, 41.3, 29.4, 19.9, 13.7. MS (APSI+) *m/z* found, 404.25; HRMS (ESI) m/z found, 404.1640; $C_{20}H_{26}N_3O_4S$ ($M^+$ + H) expected, 404.1645.

5.1.2.3. 4-(3-Butyl-2-oxoimidazolidin-1-yl)-*N*-(3-methoxyphenyl)benzenesulfonamide (**4**). Flash chromatography (Hex to Hex/EtOAc (50:50)). Yield, 73%; white solid; mp: 165-167 °C. $^{1}$H NMR ($CDCl_3$): δ 7.71-7.68 (m, 3H, Ar and NH), 7.58-7.55 (m, 2H, Ar), 7.08-7.03 (m, 1H, Ar), 6.73 (brs, 1H, Ar), 6.66-6.58 (m, 2H, Ar), 3.79-3.74 (m, 2H, $CH_2$), 3.68 (s, 3H, $CH_3$), 3.51-3.46 (m, 2H, $CH_2$), 3.28 (t,

2H, J = 7.2 Hz, $CH_2$), 1.57-1.47 (m, 2H, $CH_2$), 1.38-1.24 (m, 2H, $CH_2$), 0.90 (t, 3H, J = 7.2 Hz, $CH_3$). $^{13}C$ NMR ($CDCl_3$): δ 160.2, 157.2, 144.5, 138.3, 131.4, 129.9, 128.4, 116.1, 113.5, 110.7, 107.0, 55.2, 43.7, 42.1, 41.4, 29.4, 19.9, 13.7. MS (APSI+) *m/z* found, 404.20; HRMS (ESI) m/z found, 404.1640; $C_{20}H_{26}N_3O_4S$ ($M^+$ + H) expected, 404.1645.

5.1.2.4. 4-(3-Butyl-2-oxoimidazolidin-1-yl)-*N*-(3-fluorophenyl)benzenesulfonamide (**5**). Flash chromatography (Hex to Hex/EtOAc (50:50)). Yield, 61%; white solid; mp: 178-180 °C. $^1H$ NMR ($CDCl_3$ and MeOD): δ 8.35 (s, 1H, NH), 7.70-7.67 (m, 2H, Ar), 7.57-7.54 (m, 2H, Ar), 7.14-7.06 (m, 1H, Ar), 6.90-6.80 (m, 2H, Ar), 6.73-6.67 (m, 1H, Ar), 3.80-3.75 (m, 2H, $CH_2$), 3.51-3.46 (m, 2H, $CH_2$), 3.26 (t, 2H, J = 7.2 Hz, $CH_2$), 1.55-1.46 (m, 2H, $CH_2$), 1.37-1.25 (m, 2H, $CH_2$), 0.89 (t, 3H, J = 7.2 Hz, $CH_3$). $^{13}C$ NMR ($CDCl_3$ and MeOD): δ 164.6, 161.3, 157.2, 144.6, 131.2, 130.4, 130.3, 128.3, 116.3, ~~116.3~~, 116.2, 116.1, 111.5, 111.2, 108.1, 107.8, 43.6, 42.1, 41.3, 29.3, 19.9, 13.7. MS (APSI+) *m/z* found, 392.20; HRMS (ESI) m/z found, 392.1442; $C_{19}H_{23}FN_3O_3S$ ($M^+$ + H) expected, 392.1445.

5.1.2.6. *N*-(3-Bromophenyl)-4-(3-butyl-2-oxoimidazolidin-1-yl)benzenesulfonamide (**6**). Flash chromatography (Hex to Hex/EtOAc (50:50)). Yield, 49%; white solid; mp: 184-186 °C. $^1H$ NMR ($CDCl_3$ and MeOD): δ 7.65-7.63 (m, 2H, Ar), 7.54-7.51 (m, 2H, Ar), 7.19 (brs, 1H, Ar), 7.10-7.07 (m, 1H, Ar), 6.98-6.97 (m, 2H, Ar), 3.78-3.72 (m, 2H, $CH_2$), 3.47-3.42 (m, 2H, $CH_2$), 3.21 (t, 2H, J = 7.2 Hz, $CH_2$), 1.52-1.42 (m, 2H, $CH_2$), 1.34-1.22 (m, 2H, $CH_2$), 0.87 (t, 3H, J = 7.2 Hz, $CH_3$). $^{13}C$ NMR ($CDCl_3$ and MeOD): δ 157.2, 144.5, 138.8, 131.3, 130.4, 128.1, 127.3, 123.4, 122.5, 119.0, 116.4, 43.5, 42.1, 41.3, 29.3, 19.8, 13.6. MS (APSI+) *m/z* found 452.15; HRMS (ESI) m/z found, 452.0634; $C_{19}H_{23}BrN_3O_3S$ ($M^+$ + H) expected, 452.0644.

5.1.2.7. 4-(3-Butyl-2-oxoimidazolidin-1-yl)-*N*-(3-iodophenyl)benzenesulfonamide (**7**). Flash chromatography (Hex to Hex/EtOAc (50:50)). Yield, 44%; white solid; mp: 202-204 °C. $^1H$ NMR ($CDCl_3$ and MeOD): δ 7.66-7.63 (m, 2H, Ar), 7.56-7.53 (m, 2H, Ar), 7.38 (brs, 1H, Ar), 7.31-7.29 (m,

1H, Ar), 7.04-7.01 (m, 1H, Ar), 6.88-6.83 (m, 1H, Ar), 3.79-3.74 (m, 2H, $CH_2$), 3.49-3.44 (m, 2H, $CH_2$), 3.23 (t, 2H, J = 7.2 Hz, $CH_2$), 1.53-1.43 (m, 2H, $CH_2$), 1.35-1.23 (m, 2H, $CH_2$), 0.88 (t, 3H, J = 7.2 Hz, $CH_3$). $^{13}$C NMR ($CDCl_3$ and MeOD): δ 157.2, 144.5, 133.4, 131.3, 130.5, 129.6, 129.3, 128.2, 119.7, 116.4, 94.1, 43.6, 42.1, 41.3, 29.3, 19.9, 13.6. MS (APSI+) *m/z* found 500.10; HRMS (ESI) m/z found, 500.0499; $C_{19}H_{23}IN_3O_3S$ ($M^+$ + H) expected, 500.0506.

5.1.2.8. 4-(3-Butyl-2-oxoimidazolidin-1-yl)-*N*-(3,4-dimethoxyphenyl)benzenesulfonamide (**8**). Flash chromatography (Hex to Hex/EtOAc (50:50)). Yield, 84%; white solid; mp: 130-132 °C. $^1$H NMR ($CDCl_3$): δ 7.67 (s, 1H, NH), 7.64-7.61 (m, 2H, Ar), 7.57-7.54 (m, 2H, Ar), 6.76-6.75 (m, 1H, Ar), 6.64-6.61 (m, 1H, Ar), 6.56-6.52 (m, 1H, Ar), 3.79-3.72 (m, 8H, $CH_2$ and 2x $CH_3$), 3.51-3.46 (m, 2H, $CH_2$), 3.30-3.25 (m, 2H, $CH_2$), 1.55-1.46 (m, 2H, $CH_2$), 1.37-1.25 (m, 2H, $CH_2$), 0.89 (t, 3H, J = 7.3 Hz, $CH_3$). $^{13}$C NMR ($CDCl_3$): δ 157.3, 149.0, 147.0, 144.3, 131.3, 130.1, 128.5, 116.0, 115.4, 111.2, 107.8, 55.9, 55.9, 43.7, 42.1, 41.4, 29.3, 19.9, 13.7. MS (APSI+) *m/z* found 434.20; HRMS (ESI) m/z found, 434.1744; $C_{21}H_{28}N_3O_5S$ ($M^+$ + H) expected, 434.1750.

5.1.2.9. 4-(3-Butyl-2-oxoimidazolidin-1-yl)-*N*-(3,4-difluorophenyl)benzenesulfonamide (**9**). Flash chromatography (Hex to Hex/EtOAc (50:50)). Yield, 51%; white solid; mp: 204-206 °C. $^1$H NMR ($CDCl_3$ and MeOD): δ 7.71-7.45 (m, 5H, Ar and NH), 6.92-6.81 (m, 2H, Ar), 6.72-6.65 (m, 1H, Ar), 3.73-3.68 (m, 2H, $CH_2$), 3.47-3.41 (m, 2H, $CH_2$), 3.19-3.17 (m, 2H, $CH_2$), 1.48-1.38 (m, 2H, $CH_2$), 1.29-1.16 (m, 2H, $CH_2$), 0.89-0.80 (m, 3H, $CH_3$). $^{13}$C NMR ($CDCl_3$ and MeOD): δ 157.2, 145.6, 144.4, 144.4, 131.1, 131.1, 130.6, 129.6, 129.6, 128.1, 128.1, 117.4, 117.3, 117.3, 117.2, 117.2, 116.3, 116.3, 116.3, 116.2, 116.1, 111.0, 110.7, 43.5, 42.1, 41.2, 29.2, 19.8, 19.8, 13.5, 13.5. MS (APSI+) *m/z* found 410.20; HRMS (ESI) m/z found, 410.1343; $C_{19}H_{22}F_2N_3O_3S$ ($M^+$ + H) expected, 410.1351.

5.1.2.10. 4-(3-Butyl-2-oxoimidazolidin-1-yl)-*N*-(3,5-dimethoxyphenyl)benzenesulfonamide (**10**). Flash chromatography (Hex to Hex/EtOAc (50:50)). Yield, 73%; white solid; mp: 177-179 °C. $^1$H NMR

($CDCl_3$): δ 8.00 (s, 1H, NH), 7.71-7.68 (m, 2H, Ar), 7.55-7.52 (m, 2H, Ar), 6.28 (s, 2H, Ar), 6.11 (s, 1H, Ar), 3.76-3.71 (m, 2H, $CH_2$), 3.64 (s, 6H, 2x $CH_3$), 3.49-3.43 (m, 2H, $CH_2$), 3.26 (t, 2H, J = 7.2 Hz, $CH_2$), 1.45-1.45 (m, 2H, $CH_2$), 1.37-1.25 (m, 2H, $CH_2$), 0.89 (t, 3H, J = 7.2 Hz, $CH_3$). $^{13}$C NMR ($CDCl_3$): δ 161.1, 157.2, 144.5, 139.0, 131.3, 128.3, 116.2, 99.0, 96.8, 55.3, 43.6, 42.1, 41.3, 29.3, 19.9, 13.7. MS (APSI+) *m/z* found 434.25; HRMS (ESI) m/z found, 434.1739; $C_{21}H_{28}N_3O_5S$ ($M^+$ + H) expected, 434.1750.

5.1.2.11. 4-(3-Butyl-2-oxoimidazolidin-1-yl)-*N*-(3,5-difluorophenyl)benzenesulfonamide (**11**). Flash chromatography (Hex to Hex/EtOAc (50:50)). Yield, 7%; white solid; mp: 183-185 °C. $^1$H NMR ($CDCl_3$): δ 7.88 (s, 1H, NH), 7.77-7.74 (m, 2H, Ar), 7.64-7.61 (m, 2H, Ar), 6.72-6.70 (m, 2H, Ar), 6.51-6.45 (m, 1H, Ar), 3.87-3.82 (m, 2H, $CH_2$), 3.57-3.51 (m, 2H, $CH_2$), 3.31 (t, 2H, J = 7.2 Hz, $CH_2$), 1.58-1.50 (m, 2H, $CH_2$), 1.41-1.29 (m, 2H, $CH_2$), 0.92 (t, 3H, J = 7.2 Hz, $CH_3$). $^{13}$C NMR ($CDCl_3$): δ 164.9, 164.8, 164.2, 164.0, 161.7, 161.5, 160.8, 160.7, 157.2, 156.8, 145.8, 144.8, 139.8, 136.5, 130.9, 130.7, 129.8, ~~129.8, 128.4, 116.4,~~ 116.3, ~~116.2~~, 116.1, 115.5, 115.4, 115.3, 115.2, 115.2, 106.5, 106.2, 105.8, 103.5, 103.4, 103.1, 100.2, 99.8, 99.5, 43.7, 43.7, 42.1, 41.4, 41.3, 29.4, 29.4, 20.0, 13.8, 13.7. MS (APSI+) *m/z* found 410.20; HRMS (ESI) m/z found, 410.1325; $C_{19}H_{22}F_2N_3O_3S$ ($M^+$ + H) expected, 410.1351.

5.1.2.12. 4-(3-Butyl-2-oxoimidazolidin-1-yl)-*N*-(3,5-dichlorophenyl)benzenesulfonamide (**12**). Flash chromatography (Hex to Hex/EtOAc (50:50)). Yield, 6%; white solid; mp: 198-200 °C. $^1$H NMR ($CDCl_3$/MeOD): δ 7.71-7.68 (m, 2H, Ar), 7.60-7.57 (m, 2H, Ar), 6.98 (s, 2H, Ar), 6.96 (s, 1H, Ar), 3.81-3.76 (m, 2H, $CH_2$), 3.51-3.45 (m, 2H, $CH_2$), 3.25 (t, 2H, J = 7.2 Hz, $CH_2$), 1.55-1.45 (m, 2H, $CH_2$), 1.37-1.27 (m, 2H, $CH_2$), 0.90 (t, 3H, J = 7.2 Hz, $CH_3$). $^{13}$C NMR ($CDCl_3$/MeOD): δ 156.8, 145.9, 136.3, 135.0, 130.7, 130.5, 130.2, 129.8, 116.1, 43.7, 42.2, 41.3, 29.4, 20.0, 13.8. MS (APSI+) *m/z* found 442.15; HRMS (ESI) m/z found, 442.0755; $C_{19}H_{22}Cl_2N_3O_3S$ ($M^+$ + H) expected, 442.0760.

5.1.2.13. 4-(3-Butyl-2-oxoimidazolidin-1-yl)-*N*-(3,4,5-trimethoxyphenyl)benzenesulfonamide (**13**). Flash chromatography (methylene chloride to methylene chloride/EtOAc (90:10)). Yield, 75%; white solid; mp: 177-179 °C. $^{1}$H NMR ($CDCl_3$): δ 7.85 (s, 1H, NH), 7.69-7.66 (m, 2H, Ar), 7.59-7.56 (m, 2H, Ar), 6.37 (s, 2H, Ar), 3.80-3.73 (m, 5H, $CH_2$ and $CH_3$), 3.66 (s, 6H, 2x $CH_3$), 3.52-3.47 (m, 2H, $CH_2$), 3.28 (t, 2H, J = 7.2 Hz, $CH_2$), 1.56-1.46 (m, 2H, $CH_2$), 1.37-1.25 (m, 2H, $CH_2$), 0.89 (t, 3H, J = 7.2 Hz, $CH_3$). $^{13}$C NMR ($CDCl_3$): δ 157.2, 153.3, 144.5, 135.3, 133.1, 131.3, 128.5, 116.1, 99.5, 60.9, 56.0, 43.7, 42.1, 41.4, 29.3, 19.9, 13.7. MS (APSI+) *m/z* found 464.20; HRMS (ESI+) m/z found 464.1849; $C_{22}H_{30}N_3O_6S$ ($M^+$ + H) expected, 464.1856.

## 5.2. Biology

### *5.2.1. Cell lines culture*

MCF7 human breast carcinoma and MDA-MB-231 human breast carcinoma were purchased from the American Type Culture Collection (Manassas, VA) while HaCaT primary epidermal keratinocytes were purchased from Thermo Fisher Scientific. All cell lines were cultured in high-glucose Dulbecco's minimal essential medium (DMEM, Gibco, Thermo Fisher Scientific) supplemented with 5% (MCF7 and MDA-MB-231) and 10 % (HaCaT) fetal bovine serum (FBS, Gibco, Thermo Fisher Scientific). All cells were grown at 37 °C in a 5% $CO_2$ moisture-saturated atmosphere.

### *5.2.2. Antiproliferative activity assay*

The antiproliferative activity assay was assessed using the procedure described by the National Cancer Institute for its drug screening program, with slight modifications [30]. Ninety six-well plates (Costar®) were seeded with 75 µL of the tumor cell suspension containing 3000, 3500 and 4500 cells for MCF7, MDA-MB-231 and HaCaT cells, respectively. Plates were incubated for 24 h and then the drugs freshly solubilized in DMSO at 40 mM were added in fresh medium. Thereafter, 75 µL aliquots containing a

range of concentrations of the drug according to the maximum solubility was then added to the plates and cells were incubated for 24, 36, 48 and/or 72 h. DMSO concentration was kept constant at 0.5% (v/v) to prevent any related cytoxicity. Cell growth was stopped by the addition of trichloroacetic acid to the wells (10% (w/v) final concentration) and incubated for at least 30 min at 4 °C. The supernatant was removed and the plates were washed three times with distilled water and dried overnight. Seventy five microliters of a sulforhodamine B solution (0.1% (w/v) in 1% acetic acid) were then added to each well, and the plates were incubated for 15 to 30 min at room temperature. The unbounded dye was removed by washing the plates thrice with 1% acetic acid. The dye bounded to the cells was solubilized using a 20 mM Tris base solution and incubated for a minimum of 1 h. The absorbance was read with a SpectraMax® i3x (Molecular Devices) using an optimal wavelength (530-580 nm). Data obtained from treated cells were compared to the control cell plates fixed on the treatment day and the percentage of cell growth was thus calculated for each drug. The experiments were done at least twice in triplicate. The assays were considered valid when the coefficient of variation was < 10% for a given set of conditions within the same experiment.

***5.2.3. Cell cycle progression analysis***

MCF7 cells were seeded in 6-well plates (Costar®) (1.5 x $10^5$ cells per well) and incubated in DMEM medium for 24h. The cells were treated with compound **13** (0.2 and 0.5 μM), CEU-638 (0.01 μM) and CA-4 (0.001 μM) for 24 h. DMSO (0.5%) was used as negative control while CEU-638 and CA-4 were used as positive controls. After 24 h, the cells were trypsinized, washed with PBS, resuspended in 250 μL of PBS, fixed by the addition of 750 μL of ice-cold EtOH under agitation, and stored at -20 °C. Prior to FACS analysis, the cells were washed with PBS and resuspended in 500 μL of PBS containing 2 μg/mL 4',6'-diamidino-2-phenylindole (DAPI). Cell cycle distribution of fixed cell suspensions was evaluated using an LSR II flow cytometer (BD, Biosciences, Franklin Lakes, NJ). The increasing number

of cells in G2/M phase was calculated by subtracting the cellular population of DMSO 0.5% from the cellular population treated with compound **13**, CEU-638 and CA-4.

### *5.2.4. Immunofluorescence of microtubule*

MCF7 cells were seeded at $1.5 \times 10^5$ cells per well in 6-well plates (Costar®) containing glass coverslips (22 mm x 22 mm) coated with fibronectin (10 μg/mL) and incubated for 24 h. Tumor cells were incubated either with compound **13** (0.2 μM), CEU-638 (0.01 μM) or CA-4 (0.001 μM) for 24 h. DMSO (0.5%) was used as negative control while CEU-638 and CA-4 were used as positive controls. The cells were then washed thrice with PBS and fixed with 3.7% formaldehyde in PBS for 10 min. After two washes with PBS, the cells were permeabilized with saponin (0.1% in PBS) and blocked with 3% (w/v) BSA in PBS for 45 min at 37 °C. The cells were then incubated for 2 h at room temperature with an anti-β-tubulin monoclonal antibody (clone TUB 2.1, 1:200) in a solution containing 0.1% saponin and 3% BSA in PBS. The cells were washed twice with PBS containing 0.05% Tween 20 and the nuclei were then stained using antimouse IgG Alexa Fluor 488 (Molecular Probes, Eugene, OR; 1:1000) and DAPI (1.25 ng/mL final concentration) in blocking buffer for 1 h at 37 °C. The cover slides were mounted on a microscope slide with slow fade reagent (DakoCytomation, Carpinteria, CA) before analysis under an Olympus BX51 fluorescence microscope. Images were acquired as 8 bit-tagged image format files with a Q imaging RETIGA EXI digital camera using the Image Pro Express software.

### *5.2.5. Activation of PAIB-SA 13 into its PIB-SA parental antimitotic CEU-638*

Corning® Supersomes™ Human CYP1A1 + oxidoreductase, potassium phosphate (0.5 M), and NADPH-regenerating system solutions A and B were supplied by Fisher Scientific (Toronto, ON, Canada). Briefly, compound **13** was freshly solubilized at 60 μM in $CH_3CN$. Then, 451.8 μL of purified water, 130 μL of potassium phosphate buffer, 32.5 μL of NADPH-regenerating system solution A, 6.5 μL of NADPH-regenerating system solution B, and 13 μL of the substrate (in $CH_3CN$) were mixed and

warmed to 37 °C for 5 min. The enzymatic reaction was next initiated by adding 13.75 µL of freshly thawed human Supersomes$^{TM}$ (1 nmol/mL) to the mixture. At 0, 15, 30, 60, 90, 120 and 150 min, the enzymatic reaction was stopped by adding 100 µL of MeOH. Then, the mixture was centrifuged at 12 000 g for 5 min and 20 µL of the supernatant was analyzed by HPLC-UV (Waters ACQUITY Arc System equipped with 2998 PDA detector). The mixture was eluted using a MeOH/$H_2O$ (with 0.1% formic acid) linear gradient (1.0 mL/min) on a CORTECS C18+ reversed-phase column 30 x 50 mm x 2.7 µm equipped with a CORTECS C18+ VanGuard Cartridges 2.1 x 5 mm x 2.7 µm. Wavelength was selected at 280 nm and the peaks of compound **13** and CEU-638 were confirmed by internal standards and absorbance spectra (200-600 nm).

**Acknowledgments**

We acknowledge financial support from Merck Sharpe & Dohm program from the Faculté de médecine de l'Université Laval, start-up funds from Foundation of CHU de Québec and research infrastructure program of John R. Evans Leaders Fund from Canada Foundation for Innovation (CFI). We also acknowledge financial support from studentships from the Fonds de recherche du Québec-Santé (FRQS, MAGB) and from Fonds d'enseignement et de recherche of the Faculté de pharmacie de l'Université Laval (ACCA, MZK and MAGB).

**References**

1. Torre LA, Bray F, Siegel RL, *et al.* Global cancer statistics, 2012. *CA Cancer J Clin*. 2015;65:87-108.

2. *American Cancer Society Cancer Facts & Figures 2018 Atlanta: American Cancer Society; 2018*.

3. van Vuuren RJ, Visagie MH, Theron AE, *et al.* Antimitotic drugs in the treatment of cancer. *Cancer Chemother Pharmacol*. 2015;76:1101-1112.

4. Yardley DA. Drug resistance and the role of combination chemotherapy in improving patient outcomes. *Int J Breast Cancer*. 2013;2013:137414.

5. Prenzel T, Begus-Nahrmann Y, Kramer F, *et al.* Estrogen-dependent gene transcription in human breast cancer cells relies upon proteasome-dependent monoubiquitination of histone H2B. *Cancer Res*. 2011;71:5739-5753.

6. Siegel R, DeSantis C, Virgo K, *et al.* Cancer treatment and survivorship statistics, 2012. *CA Cancer J Clin*. 2012;62:220-241.

7. Ingelman-Sundberg M. The human genome project and novel aspects of cytochrome P450 research. *Toxicol Appl Pharmacol*. 2005;207:52-56.

8. Bernhardt R. Cytochromes P450 as versatile biocatalysts. *J Biotechnol*. 2006;124:128-145.

9. Guengerich FP. Cytochrome p450 and chemical toxicology. *Chem Res Toxicol*. 2008;21:70-83.

10. Slaughter RL, Edwards DJ. Recent advances: the cytochrome P450 enzymes. *Ann Pharmacother*. 1995;29:619-624.

11. Praporski S, Ng SM, Nguyen AD, *et al.* Organization of cytochrome P450 enzymes involved in sex steroid synthesis: protein-protein interactions in lipid membranes. *J Biol Chem*. 2009;284:33224-33232.

12. Preissner SC, Hoffmann MF, Preissner R, *et al.* Polymorphic cytochrome P450 enzymes (CYPs) and their role in personalized therapy. *PloS one*. 2013;8:e82562.

13. Culhane AC, Schwarzl T, Sultana R, *et al.* GeneSigDB--a curated database of gene expression signatures. *Nucleic Acids Res*. 2010;38:D716-725.

14. McFadyen MC, Melvin WT, Murray GI. Cytochrome P450 enzymes: novel options for cancer therapeutics. *Mol Cancer Ther*. 2004;3:363-371.

15. Murray GI. The role of cytochrome P450 in tumour development and progression and its potential in therapy. *J Pathol*. 2000;192:419-426.

16. Michael M, Doherty MM. Drug metabolism by tumours: its nature, relevance and therapeutic implications. *Expert Opin Drug Metab Toxicol*. 2007;3:783-803.

17. Lohr M, McFadyen MC, Murray GI, *et al.* Cytochrome P450 enzymes and tumor therapy. *Mol Cancer Ther*. 2004;3:1503; author reply 1503-1504.

18. Bradshaw TD, Westwell AD. The development of the antitumour benzothiazole prodrug, Phortress, as a clinical candidate. *Curr Med Chem*. 2004;11:1009-1021.

19. Callero MA, Loaiza-Perez AI. The role of aryl hydrocarbon receptor and crosstalk with estrogen receptor in response of breast cancer cells to the novel antitumor agents benzothiazoles and aminoflavone. *Int J Breast Cancer*. 2011;2011:923250.

20. Taylor SJ, Demont EH, Gray J, *et al.* Navigating CYP1A induction and arylhydrocarbon receptor agonism in drug discovery. A case history with S1P1 agonists. *J Med Chem*. 2015;58:8236-8256.

21. Ma Q, Lu AY. CYP1A induction and human risk assessment: an evolving tale of in vitro and in vivo studies. *Drug Metab Dispos*. 2007;35:1009-1016.

22. Kohle C, Bock KW. Coordinate regulation of human drug-metabolizing enzymes, and conjugate transporters by the Ah receptor, pregnane X receptor and constitutive androstane receptor. *Biochem Pharmacol*. 2009;77:689-699.

23. Spink DC, Spink BC, Cao JQ, *et al.* Differential expression of CYP1A1 and CYP1B1 in human breast epithelial cells and breast tumor cells. *Carcinogenesis*. 1998;19:291-298.

24. Murray GI, Patimalla S, Stewart KN, *et al.* Profiling the expression of cytochrome P450 in breast cancer. *Histopathology*. 2010;57:202-211.

25. Vinothini G, Nagini S. Correlation of xenobiotic-metabolizing enzymes, oxidative stress and NFkappaB signaling with histological grade and menopausal status in patients with adenocarcinoma of the breast. *Clin Chim Acta*. 2010;411:368-374.

26. Rodriguez M, Potter DA. CYP1A1 regulates breast cancer proliferation and survival. *Mol Cancer Res*. 2013;11:780-792.

27. Fortin S, Charest-Morin X, Turcotte V, *et al.* Activation of phenyl 4-(2-oxo-3-alkylimidazolidin-1-yl)benzenesulfonates prodrugs by CYP1A1 as new antimitotics targeting breast cancer cells. *J Med Chem*. 2017;60:4963-4982.

28. Fortin S, Wei L, Moreau E, *et al.* Design, synthesis, biological evaluation, and structure-activity relationships of substituted phenyl 4-(2-oxoimidazolidin-1-yl)benzenesulfonates as new tubulin inhibitors mimicking combretastatin A-4. *J Med Chem*. 2011;54:4559-4580.

29. Fortin S, Wei L, Moreau E, *et al.* Substituted phenyl 4-(2-oxoimidazolidin-1-yl)benzenesulfonamides as antimitotics. Antiproliferative, antiangiogenic and antitumoral activity, and quantitative structure-activity relationships. *Eur J Med Chem*. 2011;46:5327-5342.

30. *National Cancer Institute (NCI/NIH), Developmental therapeutics program human tumor cell line screen, URL : https://dtpcancergov/discovery_development/nci-60/defaulthtm, [accessed May 23, 2017]*.

Highlights

- PAIB-SAs are new antimitotic prodrugs
- PAIB-SAs exhibit antiproliferative activity in the submicromolar range in MCF7
- PAIB-SA **13** shows a selectivity ratio of 372 between MCF7 and HaCaT cells
- PAIB-SA **13** blocks the cell cycle in G2/M phase and disrupts microtubules
- PAIB-SA **13** is metabolized by CYP1A1 into its parental antimitotic CEU-638

Graphical abstract

**4-(3-Alkyl-2-oxoimidazolidin-1-yl)-*N*-phenylbenzenesulfonamides as new antimitotic prodrugs activated by cytochrome P450 1A1 in breast cancer cells**

Atziri Corin Chavez Alvarez, Mitra Zarifi Khosroshahi, Marie-France Côté, Mathieu Gagné-Boulet and Sébastien Fortin*